Journal of Undergraduate Chemistry Research, **2021**,20(4), 73

LOW ENERGY CONFORMATIONS OF AZELAIC ACID IN THE GAS PHASE AND IN DMSO: A B3LYP-D3 STUDY

Alina Huang*, Sabina Kalata*, Simona Risteska*, Ruben D. Parra†

Department of Chemistry and Biochemistry, DePaul University, Chicago, IL 60614

Abstract

Following a conformational search, a total of twenty three distinct low energy conformations of azelaic acid were optimized in the gas phase using the B3LYP-D3/6-311+G(2d,p) theoretical model. Eight conformers exhibit a linear (all *trans*) backbone, while fifteen conformers adopt a folded backbone that facilitates the formation of intramolecular O-H…O and C-H…O hydrogen bonds. In the gas phase, all conformers have Gibbs free energies within 2.11 kcal/mol of the most stable one. Interestingly, the two most stable conformers in the gas phase have almost identical Gibbs free energy, although one is a folded conformer while the other is a linear one. Fourteen conformers (more than half of all the conformers considered) have Gibbs free energies within 1.00 kcal/mol of the most stable one. The results of this work show that the folded conformers account for 56.6% of the corresponding Boltzmann distribution of all the conformers considered in the gas phase. To examine the effect of the environment, further geometry optimizations were carried out in DMSO for all conformers using the same theoretical model. The optimized geometries in DMSO show the conformers to be more stable than the linear counterparts. In solution, the Gibbs free energy of the least stable linear conformer lies 1.60 kcal/mol above the most stable conformer. In sharp contrast to the gas-phase results, the Gibbs free energies for all the folded conformations are much higher than those of the most stable linear conformations, i.e. between 3.35 and 6.25 kcal/mol higher than the most stable linear conformer. Solvation brings about an increase in the Boltzmann weighted average dipole moment of azelaic acid from 2.50 D in the gas phase to 3.53 D in DMSO. Lastly, the Gibbs free energy of solvation is predicted to be a favorable process with a calculated value of -14.95 kcal/mol.

†corresponding author: rparra1@depaul.edu

Keywords: azelaic acid; nonanedioic acid; conformations; hydrogen bonding; dicarboxylic acid.

Introduction

Nonanedioic acid (HOOC-$(CH_2)_7$-COOH), commonly known as azelaic acid, contains two carboxylic acid groups, COOH, linked through a backbone chain of seven methylene groups, CH_2. Given its many rotable bonds, azelaic acid may exist in hundreds, even thousands of minimum energy conformations [1, 2]. Indeed, several conformations around a single C-C bond are possible, and in particular, for *n* sp^3-sp^3 bonds in a molecule, there are 3^n possible minima. For example, there are 729 possible minima considering only the six single C-C bonds present in the backbone chain of azelaic acid. It is implied that to each of these conformations, additional conformations exist from the independent rotations in each of the two COOH groups of the molecule, namely the rotations about the sp^3-sp^2 C-C single bond and the rotations of the O-H bond around the corresponding O-C single bond.

Many molecular properties depend on the conformation adopted by the molecule. For example, a molecule may be polar in one conformation and yet non-polar in another conformation. Accordingly, an experimentally measured molecular property corresponds to the weighted average of the values of the property contributed by all the conformations at the given experimental conditions [1-5]. Among its various applications, azelaic acid has the potential to be used as a general antitumor agent, and it has actually been used to treat acne [6, 7]. There is, therefore, a fundamental motivation to determine the various conformations that azelaic acid may adopt. However, to obtain exhaustively all the possible conformations of a molecule becomes intractable for large molecules given their exponentially increasing number of rotable bonds. In general, of the potentially large number of molecular conformations only those conformers that are relatively low-energy minima contribute significantly to the observed molecular properties at some given conditions. Accordingly, changing experimental conditions such as a change in temperature may increase or decrease the number of conformations that can contribute to the average value of the molecular property of interest. A change in the physical state of the molecular system, i.e. solid to gas, may also change the number and even the type of relevant conformations. Similarly, in a liquid solution, a molecule may be more likely to adopt conformations that are best suited for interactions with solvent molecules, conformations that would otherwise be less dominant in the absence of such interactions, like in the gas phase for example.

In this study, the molecular geometries and relative energies of several low-energy local minima of azelaic acid computed *ab initio* in the gas phase are reported. The effect of the medium is also examined by considering azelaic acid in solution using DMSO as the solvent. Previous experimental work has demonstrated that azelaic acid can exist at least in two different crystal forms, namely a metastable α form and a stable β form [8, 9]. The solubility of these two polymorphs in a variety of solvents, including supercritical carbon dioxide, has been the subject of experimental investigation as well [10-13]. Theoretical calculations using the B3LYP/6-311++G(d,p) method have also been carried out to investigate the ground state geometry and molecular vibrations of the azelaic acid monomer and dimer using the X-ray structure of the _ form as an initial guess for the theoretical gas phase calculations [14]. Quite recently, our group reported an *ab inito* study on a folded conformation of azelaic acid in the gas phase at the HF and the MP2 molecular orbital methods along with the 6-311+G(2d,p) basis set [15]. The study revealed the importance of including correlation effects in determining the geometries and assessing the relative energies of azelaic acid conformations. For example, at the HF level the folded conformation is less stable than a linear conformation, while at the MP2 method the opposite is true. We are not aware of any study devoted to explore systematically the conformational space of azelaic acid in the gas phase. It is worth noting, however, that some computational studies do exist that examine the conformational stability of the smaller dicarboxylic

acids, HO_2C-$(CH_2)_n$-CO_2H (n =1-4), both in the gas phase and in the aqueous phase [16, 17]. The solvation and conformational dynamics of dicarboxylic suberic acid, which is only one methylene short from azelaic acid, was investigated using molecular dynamics simulations in water and methanol [18].

Methodology

The GMMX facility in the Gauss View program was used for the azelaic acid conformational search [19]. In particular, the MMFF94 force field was chosen for the search. All other computations were performed with the Gaussian 16 program [20]. Gas phase geometry optimizations were performed on all GMMX conformations using the B3LYP-D3 theoretical methods along with the 6-311+G(2d,p) basis set. Further geometry optimizations of the conformations were carried out in DMSO solution using the SMD method [21], and the B3LYP-D3/6-311+G(2d,p) theoretical model. Frequency calculations confirmed that each optimized structure was a local minimum with no imaginary frequencies. Relative Gibbs free energies were used to determine the relative abundance of the conformers both in gas phase and in solution. The Gibbs free energies were also used to compute the solvation energy associated with each conformer.

It is generally known that density functional methods incorrectly account for dispersion interactions, and recently there has been a trend to use empirical dispersion corrections such as the D3 to improve the accuracy of DFT relative energies, with minor additional computational cost [22, 23]. Specifically, the B3LYP-D3 functional adds to the B3LYP hybrid functional the D3 version of Grimme's dispersion term with the original D3 damping function. The importance of dispersion forces in the relative stability of azelaic acid conformations has been recently reported [15], and thus B3LYP-D3 represents a better choice in this regard over the plain B3LYP hybrid functional. The D3 dispersion correction to B3LYP is requested via the keyword EmpiricalDispersion=GD3 in the route section of the Gaussian 16 input file.

Results and Discussion

GMMX Conformational Search

First the x-ray structures of the α and β forms of solid azelaic acid were used as convenient input geometries for geometry optimizations using the B3LYP-D3/6-311+G(2d,p) model [8, 9]. Both the α and β forms are linear conformations of azelaic acid. In particular, the α form crystallizes in $P2_1/c$ and the β form crystallizes in C2/c. Then, the optimized structure of the α form was used to carry out the conformational search with the GMMX facility and the MMFF94 force field within window energies of 3.5 (the default value), 4.5, and 5.25 kcal/mol, which resulted in 20, 36 and 48 conformations respectively. All the conformations resulting from the two lower energy windows were folded structures containing intramolecular O-H…O (and some C-H…O) hydrogen bonds. Of the conformations found using the 5.25 kcal/mol window, five lack any intramolecular hydrogen bonds, and have the seven backbone or methlylene carbons (sp^3-hybridized carbons) in a linear all *trans* orientation. The conformational search using the optimized β form of azelaic acid rendered the same results as those using the corresponding α form. Close inspection of the 48 conformations revealed 18 duplicates, which were subsequently removed leaving 26 folded and 4 linear conformers. It is apparent that, within the energy windows used to carry out the conformational search, the GMMX program favors folded conformations over linear ones. It is likely that increasing the energy window even more for the conformational search would yield a great many more conformers, including additional linear conformers. It should be noted that the optimized α form of azelaic acid used for the GMMX search did not end up as one of the final conformers, so we added it. Three additional linear conformers were also constructed and their actual structures are discussed in the next section. Thus, in total 34 conformers (30 from the GMMX search, and the four additional linear conformers) were used for further computational studies as detailed below.

Gas-Phase Results

Geometry calculations were performed on each of the 34 conformations of azelaic acid using the B3LYP-D3/6-311+G(2d,p) model. Frequency calculations confirmed that all optimized structures are indeed minima with no imaginary frequencies. Four additional duplicates were found and then eliminated from further analysis. Table 1 summarizes the energy results for the 23 most abundant conformations, i.e. those accounting cumulatively for 99.3% of the total population of 30 conformations. For ease of discussion, the conformers are labeled AZA_n where n refers to the numerical ranking for the stability of the conformer in the gas phase at the B3LYP-D3/6-311+G(2d,p) level. The optimized geometries of the linear conformers are displayed in Figure 1, while those of the folded conformers are displayed in Figure 2. Table 1 also includes for each conformation its dipole moment as well as the pertinent Boltzmann fractional abundance, f_i, within the 23 conformers selected. Each f_i is calculated at room temperature (RT = 0.596152 kcal/mol) using the corresponding Gibbs energy rela-

Table 1. B3LYP-D3/6-311+G(2d,p) Relative Gibbs free energies (Δ*G*), fractional population (*f*), and dipole Moment (μ) for each azelaic acid conformer in vacuum.

Conformer	ΔG (kcal/mol)	f	μ (Debye)
AZA_1	0.00	0.13	2.78
AZA_2	0.04	0.12	3.04
AZA_3	0.13	0.10	2.83
AZA_4	0.20	0.09	2.34
AZA_5	0.26	0.08	2.58
AZA_6	0.28	0.08	0.38
AZA_7	0.50	0.06	2.60
AZA_8	0.53	0.05	2.76
AZA_9	0.60	0.05	2.57
AZA_10	0.68	0.04	2.42
AZA_11	0.75	0.04	3.02
AZA_12	0.93	0.03	2.80
AZA_13	0.98	0.03	2.56
AZA_14	1.00	0.02	2.35
AZA_15	1.32	0.01	2.76
AZA_16	1.32	0.01	2.37
AZA_17	1.33	0.01	3.31
AZA_18	1.49	0.01	2.58
AZA_19	1.66	0.01	2.77
AZA_20	1.74	0.01	0.27
AZA_21	1.93	0.01	2.38
AZA_22	1.98	0.00	2.93

tive to the most stable conformation (Equation 1).

$$f_i = \frac{\exp\left(-\frac{\Delta G_i}{RT}\right)}{\sum \exp\left(-\frac{\Delta G_i}{RT}\right)} \qquad (1)$$

Knowledge of the dipole moment for each conformation, μ_i, and its fractional abundance, f_i, allows for the calculation of a Boltzmann weighted average dipole moment: μ equals to 2.50 D, according to Equation 2:

$$\mu = \sum_i f_i \times \mu_i \qquad (2)$$

Figure 1. B3LYP-D3/6-311+G(2d,p) Optimized linear conformers of azelaic acid in the gas phase.

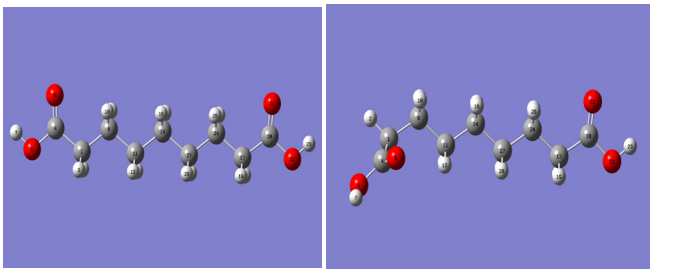

AZA_2 AZA_4

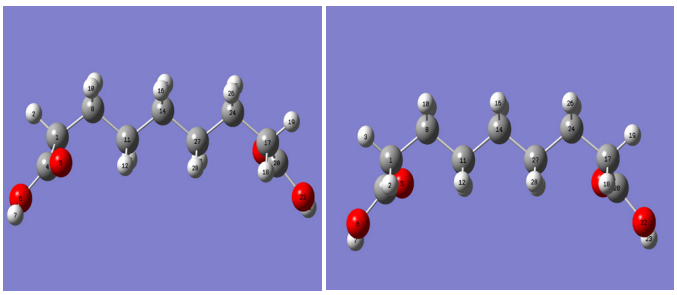

AZA_6 AZA_7

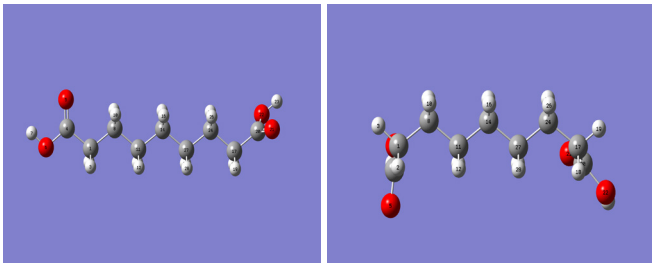

AZA_10 AZA_14

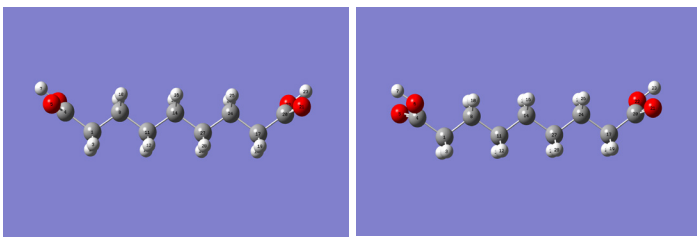

AZA_15 AZA_20

Figure 2. B3LYP-D3/6-311+G(2d,p) Optimized folded conformers of azelaic acid in the gas phase.

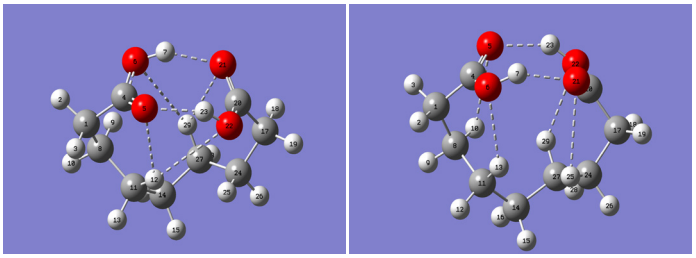

AZA_1 AZA_3

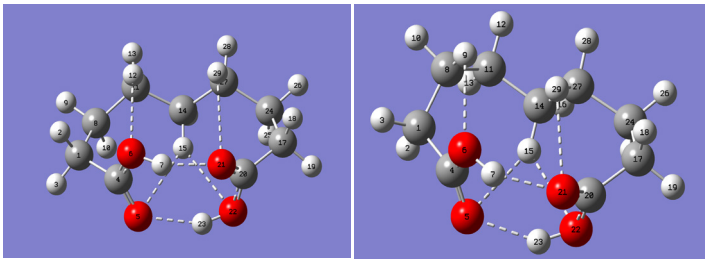

AZA_5 AZA_8

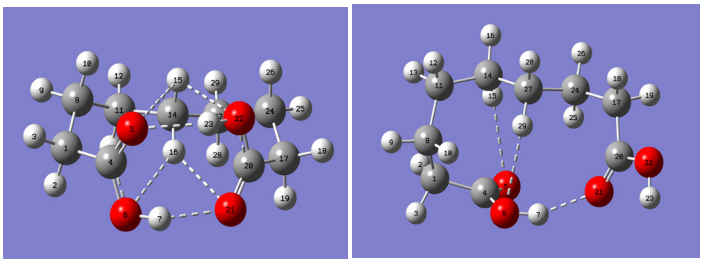

AZA_9 AZA_11

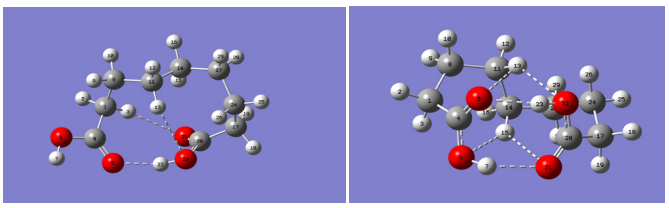

AZA_12 AZA_13

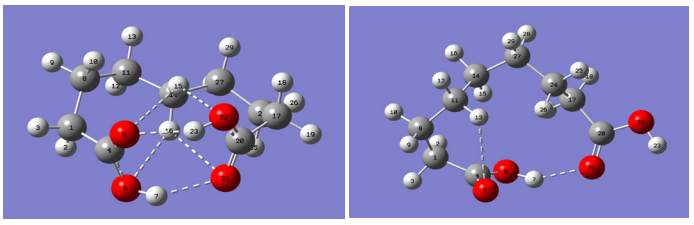

AZA_16 AZA_17

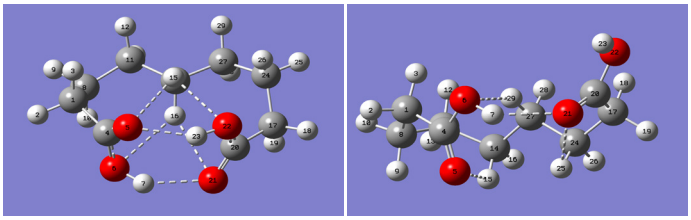

AZA_18 AZA_19

Although we did not find any peer-reviewed publication reporting the experimental dipole moment of azelaic acid, it can be noted that the calculated average dipole moment of 2.50 D is much smaller than one reported previously (6.00 D) by Kumar et al. using the B3LYP/6-311++G(d,p) in the gas phase [14]. The larger dipole moment in reference 14 was calculated for a conformation of azelaic acid that is not part of the set of 23 conformers used here. Indeed, the larger dipole moment of 6.00 D was calculated for a monomer of azelaic acid that can be derived from AZA_15 by rotating the hydrogen in OH to make it anti to the C=O bond in each carboxy group. Such conformation has a Gibbs free energy that is about 12 kcal/mol above the most stable conformation in the gas phase, AZA_1, and therefore was not included in the set of 23 most stable conformers.

Figure 2 (continued). B3LYP-D3/6-311+G(2d,p) Optimized folded conformers of azelaic acid in the gas phase.

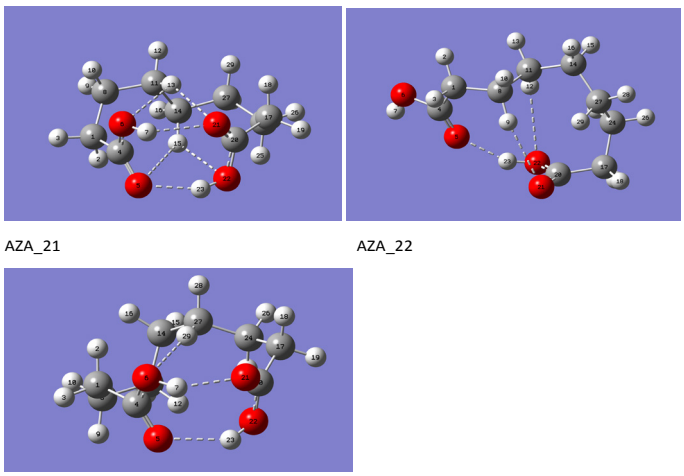

AZA_21 AZA_22

AZA_23

Table 2. Dihedral angles (in degrees) between sp^3 carbons in the B3LYP-D3/6-311+G(2d,p) optimized linear and folded conformers of azelaic acid in vacuum.

Linear Conformers

Conformer	C1-C8-C11-C14	C8-C11-C14-C27	C11-C14-C27-C24	C14-C27-C24-C17
AZA_2	180.0	180.0	180.0	180.0
AZA_4	-179.6	179.9	180.0	179.7
AZA_6	-179.5	-179.6	-179.6	-179.5
AZA_7	-179.9	179.5	-179.5	179.9
AZA_10	-179.9	-179.9	-179.9	179.8
AZA_14	-178.7	-179.4	-179.7	-179.2
AZA_15	-179.8	-180.0	180.0	179.8
AZA_20	179.8	-179.9	-179.9	179.8

Folded Conformers

Conformer	C1-C8-C11-C14	C8-C11-C14-C27	C11-C14-C27-C24	C14-C27-C24-C17
AZA_1	-152.0	81.4	81.4	-152.0
AZA_3	-155.0	76.7	76.7	-155.0
AZA_5	91.3	-167.6	172.5	-93.5
AZA_8	-65.8	-66.2	-174.5	-115.1
AZA_9	-68.4	-171.5	170.2	64.8
AZA_11	-55.4	-61.0	166.2	178.8
AZA_12	78.2	-178.8	63.4	60.4
AZA_13	46.9	170.6	59.0	68.2
AZA_16	-57.9	-167.1	-167.1	-57.9
AZA_17	56.7	-165.1	71.2	72.9
AZA_18	54.9	165.0	165.0	54.9
AZA_19	69.0	-92.9	167.4	177.3
AZA_21	58.0	172.2	101.3	-68.8
AZA_22	163.9	65.4	71.3	-133.1
AZA_23	-55.4	99.2	72.0	-154.1

Inspection of Table 1 reveals that all conformations have Gibbs free energies within 2.11 kcal/mol of the most stable conformation, AZA_1. Moreover, the first 14 conformations lie within just 1.00 kcal/mol of AZA_1 and comprise 92% of the Boltzmann distribution population. Of these 14 conformations, 8 are linear and 6 are folded conformers. Geometrical data pertaining to the dihedral angles between sp^3 carbons in the molecule are listed in Table 2, while those for the dihedral angles including the carboxy group atoms are listed in Table 3. Inspection of Table 2 makes it apparent that each of the linear conformers shows its sp^3 carbons in an all-trans orientation (dihedral angles equal or very close to 180.0°). The structural differences among the various linear conformers can be traced back essentially to different values in one or more of the dihedral angles of the corresponding carboxy groups as seen in Table 3. It should be noted that the first four linear conformers (AZA_2, AZA_4, AZA_6, and AZA_7) were found in the GMMX conformational search. AZA_2 was also obtained from the B3LYP-D3 geometry optimization of the x-ray structure of the β-form of azelaic acid. AZA_10 in turn resulted from the B3LYP-D3 geometry optimization of the x-ray structure of the α-form of azelaic acid. AZA_15 and AZA_20 were both derived from AZA_10 through full geometry optimizations using as initial guess geometries those from suitable rotations involving the O6-C4-C1-C8 and C4-C1-C8-C11 dihedral angles (Table 3). In a similar fashion, these dihedral angles were used to derive AZA_14 from AZA_7.

Table 2 shows that many of the dihedral angles between the sp^3 carbons in the folded conformers of azelaic acid tend to deviate from the *trans* conformation range towards the *gauche* conformation range. Relative to the linear conformers, changes in the dihedral angles between the sp^3 carbons along with concomitant

Table 3. Dihedral angles (in degrees) involving atoms from the carboxy group, in the B3LYP-D3/6-311+G(2d,p) optimized linear and folded conformers of azelaic acid in vacuum.

Linear Conformers

Conformer	H7-O6-C4-C1	O6-C4-C1-C8	C4-C1-C8-C11	C27-C24-C17-C20	C24-C17-C20-O22	C17-C20-O22-H23
AZA_2	180.0	180.0	180.0	180.0	180.0	180.0
AZA_4	-178.0	-167.7	70.0	179.5	179.2	179.9
AZA_6	-178.0	-167.2	70.2	70.2	-167.2	-178.0
AZA_7	178.0	166.3	-70.2	70.2	-166.3	-178.0
AZA_10	-180.0	-179.8	-179.8	-179.1	-75.0	177.8
AZA_14	179.9	-56.3	-61.3	70.2	-167.2	-178.1
AZA_15	-177.9	75.1	179.1	-179.1	-75.1	177.9
AZA_20	177.9	-75.3	-179.1	-179.1	-75.3	177.9

Folded Conformers

Conformer	H7-O6-C4-C1	O6-C4-C1-C8	C4-C1-C8-C11	C27-C24-C17-C20	C24-C17-C20-O22	C17-C20-O22-H23
AZA_1	-160.3	67.8	66.7	66.7	67.8	-160.3
AZA_3	161.2	-97.6	71.0	71.0	-97.6	161.2
AZA_5	-164.3	96.5	-48.2	48.5	70.9	-162.7
AZA_8	-166.9	60.3	79.2	50.6	56.6	-161.3
AZA_9	165.2	-123.0	64.4	-63.3	-48.5	163.1
AZA_11	-167.3	59.2	77.6	72.5	-164.9	-177.5
AZA_12	-178.4	75.1	81.6	-76.6	-58.9	168.6
AZA_13	161.6	-133.7	44.6	-74.8	-52.9	165.8
AZA_16	163.3	-125.4	71.6	71.6	-125.4	163.3
AZA_17	170.0	-126.7	45.3	-167.9	-84.5	177.0
AZA_18	163.5	-49.9	-69.6	-69.6	-49.9	163.5
AZA_19	-170.2	151.2	-75.6	73.4	-149.6	-177.3
AZA_21	-162.8	46.3	49.5	75.3	-136.8	-168.2
AZA_22	-176.9	-160.5	69.7	61.2	67.9	-164.7
AZA_23	-166.2	149.9	-58.2	61.0	58.8	-161.4

changes in the dihedral angles comprising the carboxy group atoms (Table 3) in the foldamers facilitate the formation of intramolecular O-H…O hydrogen bonds, and in many instances C-H…O hydrogen bonds as specified in Figure 2. Corresponding hydrogen bond distances and hydrogen bond angles are listed in Table 4 and Table 5 respectively. Specifically, Table 4 reveals that the O-H…O interaction distances are found to be as small as 1.743 Å (AZA_5) or as large as 2.235 Å (AZA_21). Likewise, Table 5 shows that the corresponding angles are found in the 119.9° (AZA_21) – 156.9° (AZA_12) range. The combination of large distance and large angle makes the O6-H7…O21 hydrogen bond in AZA_21 the weakest of its kind among all the conformers. Interestingly, four conformers display either one or the other of the two possible O-H…O hydrogen bonds, O6-H7…O21, and O22-H23…O5 (Figure 2). In particular, AZA_11 and AZA_17 show only the former, while AZA_12 and AZA_22 show only the latter. With an average distance of 1.921 Å and an average angle of 142.8°, all the O-H…O distances and angles fall within commonly accepted values, although the angles appear fairly deviated from the more expected linearity on account of the geometrical deformation required to bring interacting subunits together [24, 25].

Table 4. Intramolecular hydrogen bond distances, C-H…O and O-H…O (in Angstroms), in the B3LYP-D3/6-311+G(2d,p) optimized folded conformers of azelaic acid in vacuum.

Conformer	O6-H7…O21	O22-H23…O5	C-H…O5	C-H…O22	C-H…O6	C-H…O21
AZA_1	1.850	1.850	2.730	3.084	3.084	2.730
AZA_3	1.862	1.862	2.783	2.504	2.504	2.783
AZA_5	1.743	1.875	2.501	2.446	2.664	2.919
AZA_8	1.798	1.889	2.583	2.663	2.555	2.904
AZA_9	1.894	2.012	2.861	2.631	2.518	2.618
AZA_11	1.934	--	2.506	--	2.504	--
AZA_12	--	1.793	--	2.601	--	2.441
AZA_13	1.981	1.900	2.646	2.495	2.665	2.804
AZA_16	1.983	1.983	2.701	2.454	2.454	2.701
AZA_17	1.901	--	2.612	--	--	--
AZA_18	1.951	1.951	2.606	2.590	2.590	2.606
AZA_19	2.021	--	2.535	--	2.541	2.641
AZA_21	2.235	1.880	3.107	2.715	2.661	2.528
AZA_22	--	1.836	--	2.680	--	2.499
AZA_23	2.003	2.041	2.672	2.859	2.592	2.835

Table 5. Intramolecular hydrogen bond angles, C-H…O and O-H…O (in degrees), in the B3LYP-D3/6-311+G(2d,p) optimized folded. conformers of azelaic acid in vacuum

Conformer	O6-H7…O21	O22-H23…O5	C-H…O5	C-H…O22	C-H…O6	C-H…O21
AZA_1	145.2	145.2	127.3	151.3	151.3	127.3
AZA_3	144.8	144.8	96.1	128.7	128.7	96.1
AZA_5	153.3	149.1	147.1	142.9	110.4	108.6
AZA_8	149.5	142.1	141.6	128.6	99.7	121.5
AZA_9	142.9	141.0	98.3	104.9	146.5	143.8
AZA_11	147.3	--	133.8	--	137.2	--
AZA_12	--	156.9	--	138.4	--	155.4
AZA_13	132.5	142.6	110.1	143.1	142.9	137.8
AZA_16	138.7	138.7	115.3	136.2	136.2	115.3
AZA_17	150.2	--	116.8	--	--	--
AZA_18	140.6	140.6	128.1	120.9	120.9	128.1
AZA_19	137.2	--	119.3	--	149.4	94.5
AZA_21	119.9	144.3	131.7	127.6	112.1	150.8
AZA_22	--	155.0	--	131.6	--	161.0
AZA_23	134.8	131.9	113.2	154.0	168.6	126.7

A noteworthy observation based on Figure 2 is that, with only four exceptions (AZA_1, AZA_3, AZA_17, and AZA_18), the majority of the foldamers contain also some identifiable C-H…O hydrogen bonds. Table 4 reveals that the C-H…O distances are found to be as small as 2.441 Å (AZA_12) or as large as 3.107 Å (AZA_21). Likewise, Table 5 shows that the corresponding angles are found in the 94.5° (AZA_19) – 168.6° (AZA_23) range. With an average distance of 2.658 Å and an average angle of 129.1°, all the C-H…O distances and angles fall within the values commonly associated with these relatively weak hydrogen bonds [24].

Solution-Phase Results

The optimized geometries of the 23 most stable gas-phase conformations of azelaic acid were further optimized in solution using the SMD method and the polar DMSO solvent. Frequency calculations confirmed that all optimized structures are indeed minima with no imaginary frequencies. The results presented in Table 6 show that the linear conformations are the most stable ones, accounting essentially for all of the total distribution of conformations in solution. The geometrical parameters of the linear conformers change very little upon solvation. For example, the dihedral angles involving the sp^3 carbons in the molecule are essentially unchanged. More sizeable changes upon solvation are seen, however, in the dihedral angles involving the carboxy group atoms, whose values in DMSO are listed in Table 7. It is noteworthy that the three folded conformations (AZA_1, AZA_3, and AZA_5), which together account for 31.5% of the Boltzmann distribution of conformations in the gas phase, make negligible contribution to the total population in solution. The two most stable conformations in solution (AZA_10, and AZA_2) account for 65.5% of the Boltzmann distribution. It is important to recall that the AZA_2

Table 6. B3LYP-D3/6-311+G(2d,p) Relative Gibbs free energies (ΔG), fractional population (f), and dipole moment (μ) for each azelaic acid conformer in DMSO.

Conformer	ΔG (kcal/mol)	f	μ (Debye)
AZA_10	0.00	0.36	3.31
AZA_2	0.12	0.29	4.27
AZA_4	0.57	0.14	3.38
AZA_15	0.94	0.07	3.66
AZA_7	1.22	0.05	3.98
AZA_14	1.49	0.03	3.08
AZA_20	1.56	0.03	0.81
AZA_6	1.60	0.02	0.87
AZA_11	3.35	0.00	4.61
AZA_12	3.59	0.00	4.25
AZA_17	4.05	0.00	4.87
AZA_22	4.30	0.00	4.46
AZA_9	4.93	0.00	3.59
AZA_19	5.03	0.00	4.15
AZA_1	5.06	0.00	3.82
AZA_3	5.17	0.00	3.93
AZA_5	5.30	0.00	3.66
AZA_13	5.34	0.00	3.47
AZA_21	5.53	0.00	3.96
AZA_8	5.53	0.00	3.86
AZA_16	5.88	0.00	3.23
AZA_18	6.05	0.00	3.54
AZA_23	6.25	0.00	3.51

was also obtained from the B3LYP-D3 geometry optimization of the x-ray structure of the β-form of azelaic acid, and that AZA_10 in turn resulted from the B3LYP-D3 geometry optimization of the x-ray structure of the α-form of azelaic acid.

The individual dipole moments for the various conformations listed in Table 6 are used to obtain a corresponding Boltzmann weighted average dipole moment for azelaic acid in solution, μ equals to 3.53 D, according to Equation 2. Thus, an increase of 1.03 D, relative to the gas phase value (2.50 D), is calculated for the dipole moment of this molecule upon solvation in DMSO. Changes of solute electronic structure properties, relative to gas phase values, are expected upon solvation of the solute, and the magnitude of these changes correlates with the strength of the interactions [3, 4]. In particular, dipole moments in solution are expected to be larger than pertinent dipole moments in the gas phase.

Table 7. Dihedral angles (in degrees) involving atoms from the carboxy group, in the B3LYP-D3/6-311+G(2d,p) optimized linear conformer of azelaic acid in DMSO.

Conformer	H7-O6-C4-C1	O6-C4-C1-C8	C4-C1-C8-C11	C27-C24-C17-C20	C24-C17-C20-O22	C17-C20-O22-H23
AZA_2	180.0	180.0	180.0	180.0	180.0	180.0
AZA_4	-176.9	-157.7	70.1	179.9	-179.3	-179.9
AZA_6	-176.8	-154.8	69.9	69.9	-154.8	-176.8
AZA_7	176.9	156.7	-69.9	69.9	-156.7	-176.9
AZA_10	-179.8	-178.9	179.8	-178.7	-81.4	177.2
AZA_14	179.6	-58.9	-61.5	69.7	-156.4	-176.9
AZA_15	-177.1	84.0	179.0	-178.6	-78.5	177.4
AZA_20	177.2	-82.0	-178.6	-178.6	-82.0	177.2

Table 8. B3LYP-D3/6-311+G(2d,p) Gibbs free energies (in gas phase and in DMSO solution) and corresponding solvation energies, Δ*G*, for each azelaic acid conformer.

	DMSO	Gas	Solvation
Conformer	***G* (Hartrees)**	***G* (Hartrees)**	**Δ*G* (kcal/mol)**
AZA_10	-653.604521	-653.579796	-15.52
AZA_2	-653.604328	-653.580819	-14.75
AZA_4	-653.603615	-653.580565	-14.46
AZA_15	-653.603018	-653.578780	-15.21
AZA_7	-653.602575	-653.580084	-14.11
AZA_14	-653.602150	-653.579291	-14.34
AZA_20	-653.602040	-653.578122	-15.01
AZA_6	-653.601979	-653.580443	-13.51
AZA_11	-653.599177	-653.579695	-12.23
AZA_12	-653.598806	-653.579411	-12.17
AZA_17	-653.598074	-653.578768	-12.11
AZA_22	-653.597670	-653.577739	-12.51
AZA_9	-653.596660	-653.579937	-10.49
AZA_19	-653.596504	-653.578241	-11.46
AZA_1	-653.596456	-653.580887	-9.770
AZA_3	-653.596277	-653.580687	-9.783
AZA_5	-653.596068	-653.580479	-9.782
AZA_13	-653.596019	-653.579331	-10.47
AZA_21	-653.595709	-653.577818	-11.23
AZA_8	-653.595704	-653.580040	-9.829
AZA_16	-653.595157	-653.578779	-10.28
AZA_18	-653.594882	-653.578508	-10.27
AZA_23	-653.594566	-653.577525	-10.69

This increase of dipole moment is clearly predicted for azelaic acid in DMSO, and the extent of the increase (41% increase) reveals significant solute-solvent interactions.

Free Energy of Solvation

The SMD method used for the geometry optimization and frequency calculations of azelaic acid in solution is also a recommended approach for computing free energy of solvation [4, 21]. With this method, the free energy of solvation is obtained as a free energy of transfer from gas phase into solution, at 298.15 K and a 1 M concentration for both the gas phase and the solution phase. The difference of the predicted Gibbs free energies of a fully optimized azelaic acid conformation both in the gas phase and in DMSO is the corresponding free energy of solvation, $\Delta G_{Solv,i}$, as shown in Table 8. The negative sign for the free energy of solvation shows that the transfer of the solute molecule into the polar condensed phase offered by the DMSO solvent is a favorable process. The magnitude of $\Delta G_{Solv,i}$ is larger for the linear azelaic conformers (ranging between -13.51 and -15.52 kcal/mol) than for the linear conformers (ranging between -9.77 and 12.17 kcal/mol). The Boltzmann distribution of the conformations in solution (Table 6) leads to a weighted average ΔG_{Solv} equals to -14.95 kcal/mol. As expected, the weighted average value for ΔG_{Solv} reflects more the contributions of the individual linear rather than those of the folded conformers. We were unable to find experimental values for the free energy of solvation of azelaic from the gas phase into solution to compare with.

Conclusions

The results of this work show that a number of low energy conformations exist for azelaic acid. Specifically, 23 different conformations were presented and discussed in this work. Fifteen conformations exhibit a folded conformation while the remaining eight have a linear conformation. Folded conformations display intramolecular C-H…O and O-H…O hydrogen bonds, whereas the linear conformations do not. The Boltzmann distribution of the conformations is found to depend on the environment. In the gas phase, for example, the folded conformations account for 56.6% of the Boltzmann distribution. In DMSO solution, however, the linear conformations accounts for 99.6% of the Boltzmann distribution. These results reveal the role played by the solvent molecules disrupting the rather weak intramolecular hydrogen bonding and replacing them with stronger intermolecular interactions, including intermolecular hydrogen bonding. Thus, the energetic stabilization resulting from favorable intermolecular interactions of the linear conformers with the solvent accounts for their corresponding dominant Boltzmann distribution in solutions. The weighted average dipole moment of azelaic acid increases from 2.50 D in the gas phase to 3.53 D in DMSO. Lastly, the weighted Gibbs free energy of solvation, ΔG_{solv}, is calculated to be -14.95 kcal/mol. That is, solvation appears to be thermodynamically favorable. Experimental work is required to assess the reliability of the predicted ΔG_{solv} given here. Building on our understanding of the monomer, we are currently investigating *ab initio* the formation of azelaic acid aggregates like dimers, trimers, and tetramers. The results of this ongoing research will be published elsewhere.

Acknowledgement

We send our special thanks to the Department of Chemistry and Biochemistry at DePaul University for its continuous support for research in general and in particular for research involving undergraduate students.

References

(1) Rappé, A. K.; Casewit, C. J. *Molecular Mechanics across Chemistry*, University Science Books, Sausalito, CA, **1997** pp. 20-27.
(2) Dodziuk, H. *Modern Conformational Analysis: Elucidating Novel Exciting Molecular Structures*, VCH Publishers, Inc., New York, NY, **1995** pp. 10-20.
(3) Cramer, C. J. *Essentials of Computational Chemistry: Theories and Models*, 2nd Ed. Wiley, Chichester, West Sussex, England, **2004**, pp. 377-393.
(4) Foresman, J. B.; Frish, Æ. *Exploring Chemistry with Electronic Structure Methods*, 3rd Ed. Gaussian, Inc. Wallingford, CT, **2015**, pp.164-225.
(5) Cruz-Cabeza, A. J.; Bernstein, *J. Chem. Rev.*, **2014**, 114, 2170−2191.
(6) Breathnach, A. S. *Med. Hypotheses*, **1999**, 52, 221–22.
(7) Young, M.C.; Zito, P. M. *J. Dermatol. Nurses Assoc.*, **2018**, 10, 152-153.
(8) Bond. A. D.; Edwards, M. R.; Jones, W. *Acta Cryst.*, **2001**, E57, 143-144
(9) Allen, F. H.; Kennard, O. *Chem. Des. Autom. News*, **1993**, 8, 31-37.
(10) Su, W.; Guo, P.; Zhang, Y.; Liu, X.; Hao, Q.; Wang, H.; Li, C. *J. Mol. Liq.*, **2020**, 317, 1-11.
(11) Sparks, D. L.; Hernandez, R.; Estévez, A. L.; Meyer, N.; French T. *J. Chem. Eng. Data*, **2007**, 52, 1246-1249.
(12) Zhang, H.; Yin, Q.; Liu, Z.; Gong, J.; Bao, Y.; Zhang, M.; Hao, H.; Hou, B.; Xie, C. *J. Chem. Thermodynamics*, **2014**, 77, 91-97.
(13) Zhang, H.; Xie, C.; Liu, Z.; Gong, J.; Bao, Y.; Zhang, M.; Hao, H.; Hou, B.; Yin, Q-X. *Ind. Eng. Chem. Res.*, **2013**, 52, 18458−18465.
(14) Kumar, A.; Narayan, V.; Prasad, O.; Sinha, L. J. Mol. Struct., **2012**, 1022, 81-88.
(15) Kalata, S.; Huang, A.; Parra, R. DePaul Discoveries, **2021**, 10 (1), Article 12.
(16) Nguyen, T. H.; Hibbs, D. E.; Howard, S. T. J. *Comp. Chem.*, **2005**, 26, 1233-1241.
(17) Tarakeshwar, P.; Manogaran, S. *J. Mol. Struct. (Theochem)*, **1996**, 362, 77-99.
(18) Nilsson, J. A.; Laaksonen, A.; Erikson, L. A. *J. Chem. Phys.*, **1998**, 109, 2403-2412.
(19) Dennington, R.; Keith, T. A.; Millam, J. M. GaussView, Version 6, Semichem Inc., Shawnee Mission, KS, **2016**.
(20) Frisch, M.J.; Trucks, G.W.; Schlegel, H.B.; et al. Gaussian 16, Revision A.03; Gaussian, Inc.: Wallingford, CT, USA, **2016**.
(21) Marenich, A. V.; Cramer, C. J.; Truhlar, D. G. *J. Phys. Chem. B*, 2009, 113, 6378-6396.
(22) Grimme, S.; Hansen, A.; Brandenburg, J. G.; Bannwarth, C. *Chem. Rev.*, **2016**, 116, 5105-5154.
(23) Folmsbee, D.; Hutchison, G. *Int J Quantum Chem.*, **2021**,121:e26381.
(24) Desiraju, G. R; Steiner, T. *The Weak Hydrogen Bond In Structural Chemistry and Biology*, Oxford University Press, New York, NY, **1999**, pp. 1-21.
(25) Arunan, E.; Desiraju, G. R.; Klein, R. A.; Sadlej, J.; Scheiner, S.; Alkorta, I.; Clary, D. C.; Crabtree, R. H.; Dannenberg, J. J.; Hobza, P.; Kjaergaard, H. G.; Legon A. C.; Mennucci, B.; Nesbitt, D. *Pure Appl. Chem.,* **2011**, *83*, 1637-1641.